Fast Automatized Parameter Adaption Process of CNC Milling Machines Under the Use of Perception Based Artificial Intelligence

S. Feldmann¹, M. Schmiedt¹, J. Jung¹, J. M. Schlosser¹, T. Stempfle¹, C. Rathmann¹, W. Rimkus¹

¹Hochschule Aalen, Germany

Abstract— This paper concerns unpublished results obtained from the SIMKI (2020) R&D project at the Department of Mechanical Engineering at Aalen University of Applied Science, Germany. The following text generally discusses the development results of the AI-based CNC parameter identification and optimisation tool AICNC. The identification tool supports the AI-based optimisation of milling machine process parameters when using unknown material compositions. The process parameters are determined by a specific test pattern designed to be automatically analysed in real-time by a pretrained perception-based deep learning algorithm. The tool provides the advantage of obtaining real-time quality information due to AI-based quality assessment and the automated identification of material-dependent milling process parameter sets, even for unknown processing material.

Keywords—Artificial Intelligence · CNC-Milling · Image Processing · Parameter Prediction · Process Optimisation

I. INTRODUCTION

THE manufacturing sector plays an important role in the gross domestic product (GDP) of the European Union [1]. Nowadays, companies in the metal processing industry are under constant time and cost pressure due to increasing

international competition. Furthermore, they must comply with increasingly strict documentation and environmental requirements [2], [3]. Reducing material waste and energy consumption in the production process are crucial for ensuring the future viability of industrial companies. To increase the efficiency in handling new processing materials with unknown mechanical properties, an AI-based CNC parameter optimization tool (AICNC) has been developed within the SIMKI research group at the Department of Mechanical Engineering at Aalen University [4], [5]. The software tool utilises perception-based deep neural network technology based on the SqueezeNet architecture [6]. The tool features a process to automatically predict the necessary CNC milling parameter settings, e.g. feed and rotation speed of the milling machine, by analysing predefined test patterns. Within the SIMKI research activities, a demonstrator was developed that transfers the theoretical results to an automated software tool that is applicable under industrial conditions [7]. This simple and costeffective solution significantly enhances the efficiency of CNC milling processes while reducing environmental impact by minimizing material waste.

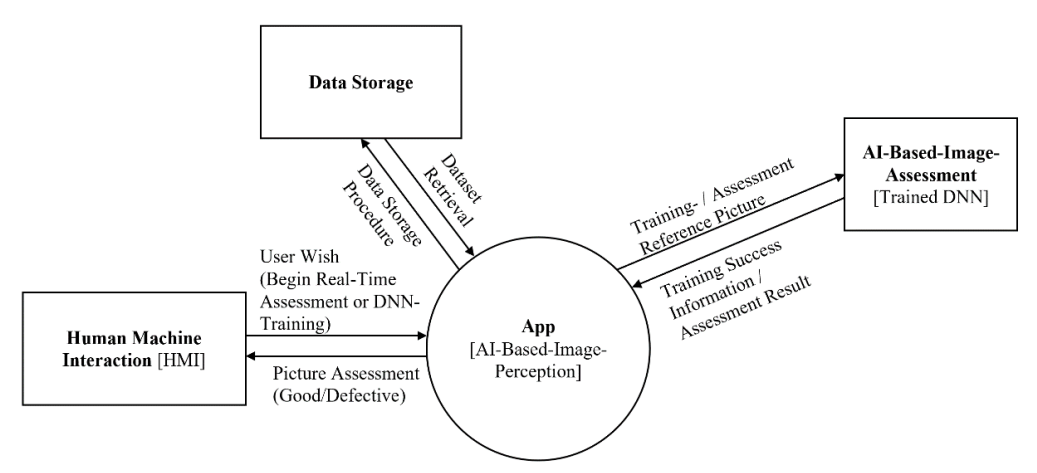


Fig. 1: AICNC software module infrastructure overview

II. GENERAL ASIC FUNCTIONAL

Fig. 1 presents an overview of the software modules and database components used in AICNC. AICNC utilizes an adapted deep learning neural network (DNN) that is trained using specific test patterns of CNC-milling sample parts such as circles or squares. The DNN can detect parts with inadequate surface or edge structures and correlate them with the feed and rotation speed settings applied.

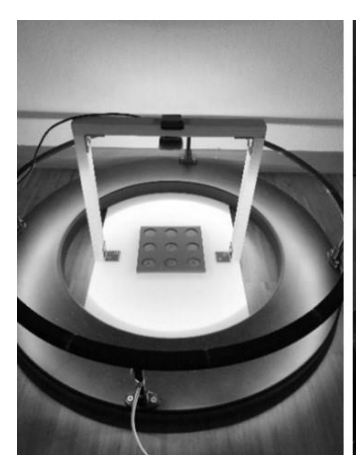




Fig. 2: Left: AICNC image acquisition hardware interface setup; right: Test pattern generation on the DMU 65 mono Block 5-axis CNC milling machine reference DMU

The user interface (HMI) has four general interaction tabs for teaching and evaluating the acquired test patterns using the built-in DNN. The application includes a semi-automated image acquisition and image cropping tool that generates training database images under constant conditions. The trained DNN can be optimized further using images created during daily production activities. The HMI interface provides the ability to capture images, train the network, and classify the best-fitting combinations of feed and rotation speed for unknown material combinations.

Table I: Test pattern milling parameter combination properties of the generic pattern generation for adaptive milling parameter identification and adaption, at the DMU65 milling machine.

_								
Generic Pattern Parameter Set-Curricular Surface								
	Cutting	Feed	Dipping	Cutting	Cooling	Milling tool		
Speed			Feed	width	Method			
	v_z	f_z	f_z	DXY				
	[m/min]	[mm/min]	[mm/min]	[%]				
1	210	802.2	30	50	Water	HM, coated 10 mm Z3		
2	210	401.1	30	50	Water	HM, coated 10 mm Z3		
3	210	1604.4	30	50	Water	HM, coated 10 mm Z3		
4	420	802.2	30	50	Water	HM, coated 10 mm Z3		
5	420	401.1	30	50	Water	HM, coated 10 mm Z3		
6	420	1604.4	30	50	Water	HM, coated 10 mm Z3		
7	105	802.2	30	50	Water	HM, coated 10 mm Z3		
8	105	401.1	30	50	Water	HM, coated 10 mm Z3		
9	105	1604.4	30	50	Water	HM, coated 10 mm Z3		

The final training and pattern assessment results are

provided using a layer activation map that indicates the correlated training features of the reference images. Additionally, the layer activation map representation can also be used for real-time inline quality control by an inline image acquisition device. This feature is discussed in further work, e.g. [12], and is not part of this paper. Fig. 2 on the left provides an overview of the acquisition infrastructure used during the test period.

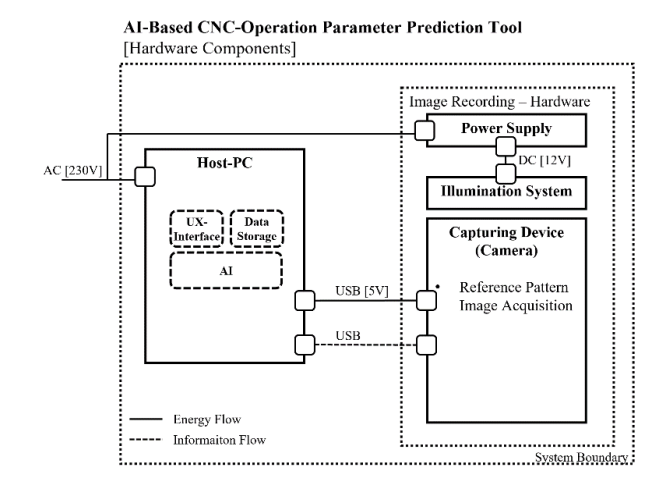


Fig. 3: Schematic AICNC hardware interfaces and component representation

The module comprises a consumer market video capture device with a resolution of 720p, a processing rate of 30 frames per second (fps), and a field of view (fov) of 68.5°. The hardware is connected to the AICNC software module at a distance of 300 mm above the test specimen. To minimize environmental impact and ensure optimal pattern recognition, a circular LED illumination system is installed around the capture area (see Fig. 2, left). Fig. 2 on the right displays a image of the test pattern generation process using the DMU65 milling machine. The test pattern comprises of nine distinct areas obtained by specific combinations of machine-related parameter settings such as feed and cutting. The procedure was applied under industrial conditions using the 5-axis CNC machining centre DMU 65 monoBlock as a reference system [8]. This method can be applied to various machines and processes in this sector. To obtain the initial machine parameter settings, a literature source was used (the machining manual [9]) to specify the material-dependent initial parameters of the milling machine. For example, the cutting speed v_c was set to 210 m/min and the feed fz was set to 802.2 mm/min. This parameter set can be safely used to obtain sufficient results, but there is room for increasing the processing speed according to the desired quality criteria. The literature provides an initial parameter set, which serves as a starting point for applying the generic pattern of AICNC. To identify the parameter set that produces optimum part quality, the test pattern is applied with eight increasing combinations of cutting speed and milling tool feed.

Table I presents the generic pattern parameter set used in the experiment to identify material-dependent processing potential

based on the predefined machine setting. No changes in content have been made. The identified potential results in increased processing speed, leading to significant time and cost savings compared to the standard parameter settings manually.

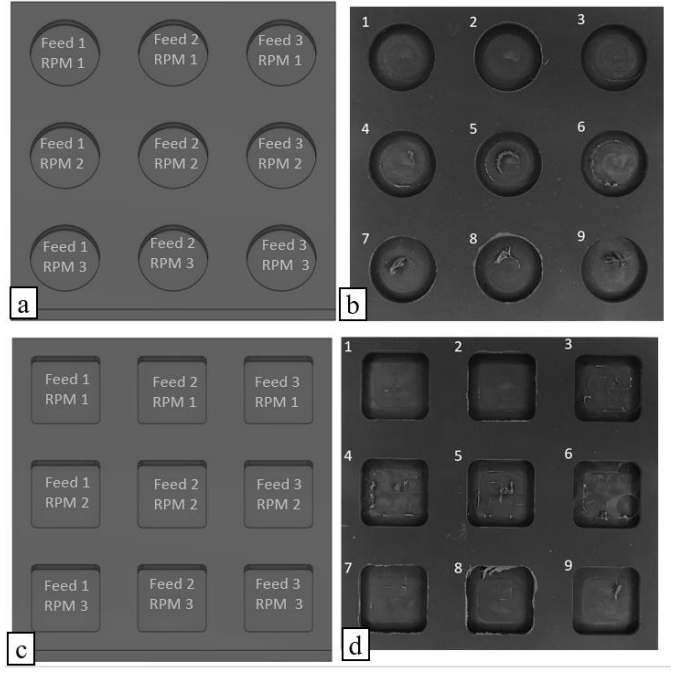


Fig. 4: a,c: AICNC test pattern model; b,d: AICNC manufactured test pattern reference sample probe

Fig. 3 shows the corresponding hardware component context and provides an overview of the communication and energy interface setup used in the experiment. The project aimed to minimize investment and integration costs by using widely available hardware components and communication interfaces. In later stages, the software-based compensation can replace the illumination system to account for environmental disturbances.



Fig. 5: "Record" tab UX-representation

Fig. 4. provides an exemplary overview of the generated test patterns and the resulting defect occurrence according to the machine parameter set of Table I. The pattern layers have a size of 140 x 140 mm and a thickness of 5 mm. The type of material

used within the development test procedures was a rigid Polyvinyl Chloride (PVC) synthetic plastic polymer. The typical material parameters are density: 1.3 to 1.45 g/cm³, thermal conductivity: 0.14 to 0.28 W/mK, and yield strength of 1450 to 3600 MPa [9]. The generic circular patterns were generated with a diameter of 30 mm and the square patterns with an edge length of 30 mm. According to the reference values found in the literature, the machine feed can be increased up to step three to obtain results of equivalent quality to step one, compare Fig. 4 – circular pattern. The same result is obtained for the square pattern. According to the square samples in pattern seven, an increased cutting speed also leads to adequate quality results.

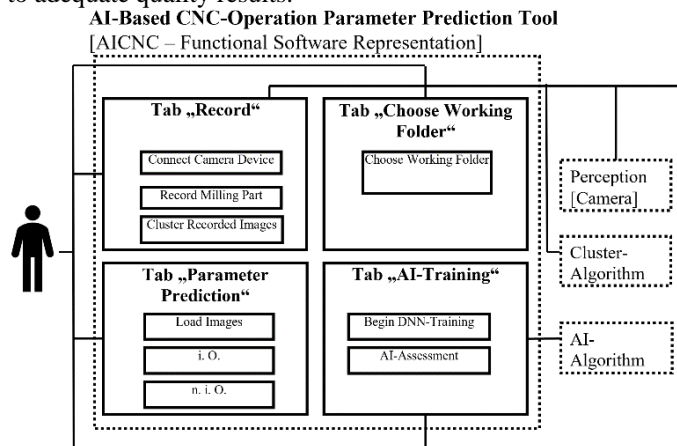


Fig. 6: AICNC HMI-interface architecture

This effect was observed during several test runs. The AI-based parameter prediction tool AICNC automatically clusters the results and stores the samples in a data space according to the good/bad AI-based assessment result. The algorithm is now able to interpolate and provide a material-specific, machine-optimized parameter set. Fig. 6 represents the pre-processed training pattern image files generated from each test run of the milling machine.

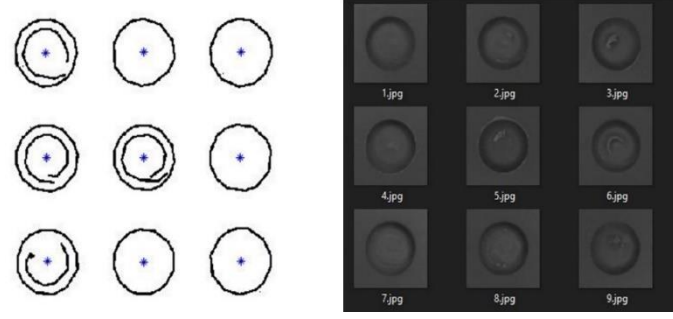


Fig. 7: Left: Generic sample pattern edge and centroid detection result right: AICNC segmented test pattern reference sample image

III. AICNC USER INTERFACE AND WORKFLOW REPRESENTATION

The AICNC user interface workflow is generally divided into four specific task tabs that guide the user through the necessary steps. The AICNC application communicates directly with the hardware-specific image acquisition and clustering methods.

Additionally, the DNN represents a separate software instance that is connected to the functional interfaces of the AI training and assessment tabs, compared to Fig. 7.

In an initial step, the user connects the desired image/video capture device at the 'record' tab. This view allows the user to capture images of the connected device. The "clustering" method performs a segmentation process that includes subroutines for image scaling, edge detection, and centroid detection. The captured images of the generic sample patterns are counted according to the centroids found by the algorithm. After the segmentation is finished, the sliced patterns are stored in a common folder. Specific working folders can be selected in the 'working folder' tab. The specified working folder contains the raw image data and the segmented training images.

The 'parameter prediction' tab is mainly a user interface that supports the manual classification process of the captured training images. The captured and segmented sample patterns are loaded and analysed by the user. The OK (good) and NOK (defective) buttons save them to the appropriate DNN training folders. Finally, the "AI-training" tab uses database images to train predefined material patterns. To increase the accuracy, different material types can be used in the DNN pre-training process. The trained deep neural network (DNN) provides a feedback value indicating whether the assessed samples meet the OK or NOK criteria. Additionally, it generates an activation map of the heat layer, highlighting the significant features of the generic sample pattern. The activation map (heat activation layer) is correlated with the backward mapping, which identifies the important image features of the damaged parts.

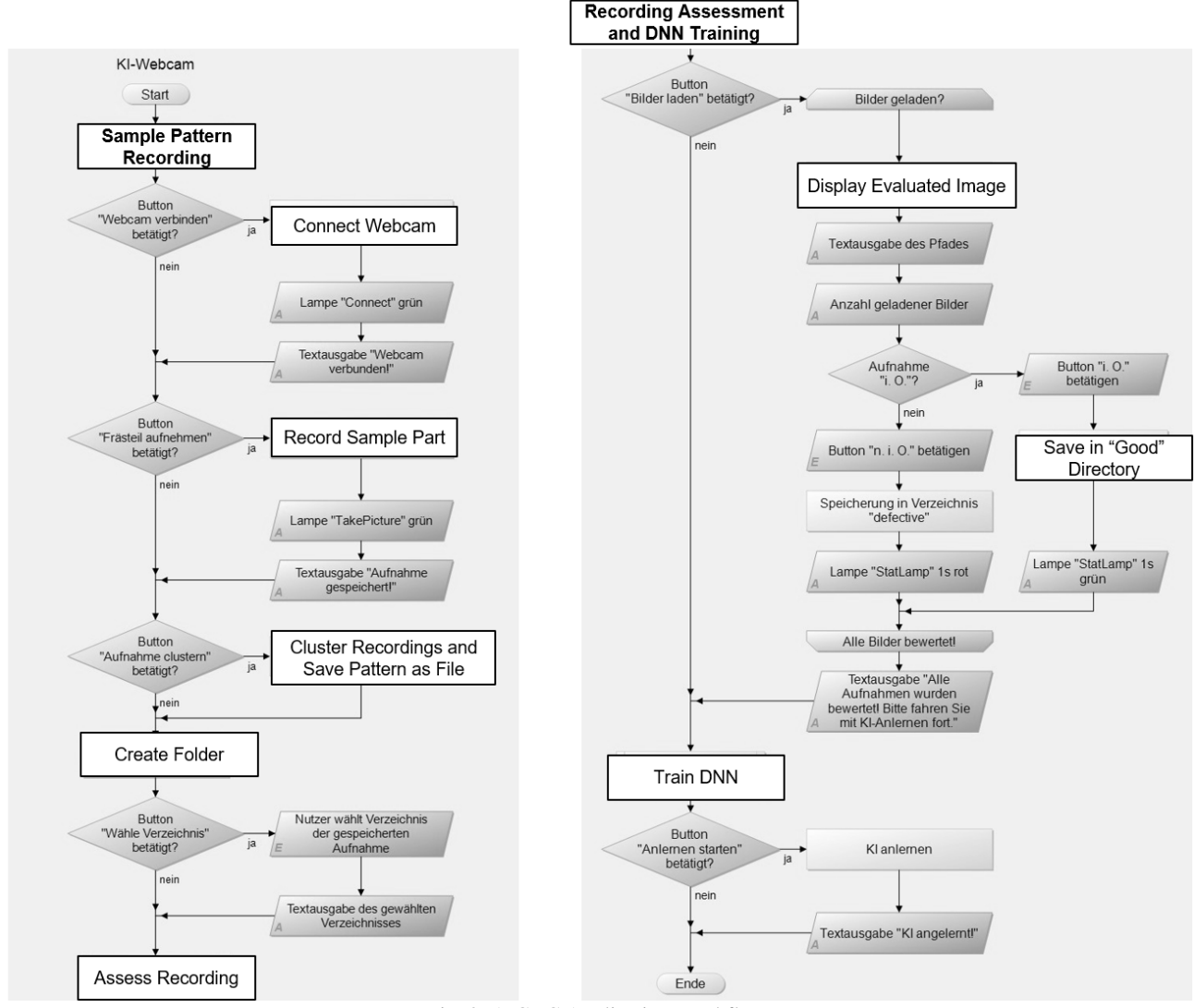


Fig. 8: AICNC Application Workflow

Fig. 7 represents the user view in the 'record' tab. Correctly captured and segmented images are indicated by green-light feedback. Additionally, a continuous system log will be created to validate the user feedback over time. This is important to

correlate differences in the detection accuracy according to the DNN training process. Fig. 9 represents the AICNC training and assessment tab. This tab provides access to software methods for the DNN training procedure. Once the training

process is complete, the system is compatible with a wide range of video capture devices. The assessment button segments the latest captured image and generates a confidential value indicating whether the captured image is OK or NOK Additionally, the activation layer display indicates the area and impact of defects according to the intensity colour overlay provided by the user interface. The usage of AICNC is divided into two main user-driven workflows. The initial workflow targets sample pattern recording and pattern slicing, comp. Fig. 8 left. Folders are automatically generated and each pattern of the recorded sample probe is sliced into square patterns and numbered by software. Labelling of each probe is done by the applicator at the second workflow, comp. Fig. 8 right. The second workflow concerns the creation of labelled image data for the DNN training process. The assessed image data will be saved in the corresponding training folders by software. DNN training environment and result validation

The DNN training procedure was performed with 30 'good' rated and 43 'defective' rated images. With 75 training iterations and 150 training epochs. The training PC includes a Core i5-7600K processor with a 3.79 GHz clock rate and 16 GB RAM. The operating system is based on WIN 10 Pro. The training was performed on a single CPU at a period of 4:22 minutes to reach a validation accuracy of 60 %. The DNN structure is based on the 'SqueezeNet' architecture with exchanged input layers. SqueezeNet is a deep neural network architecture originally developed to reduce the number of parameters and memory size compared to other neural networks, see Table II. This architecture consists of several Convolutional Layers, Max Pooling Layers, Fire Layers, a global average Layer, a Fully Connected Layer, and an Output Layer.

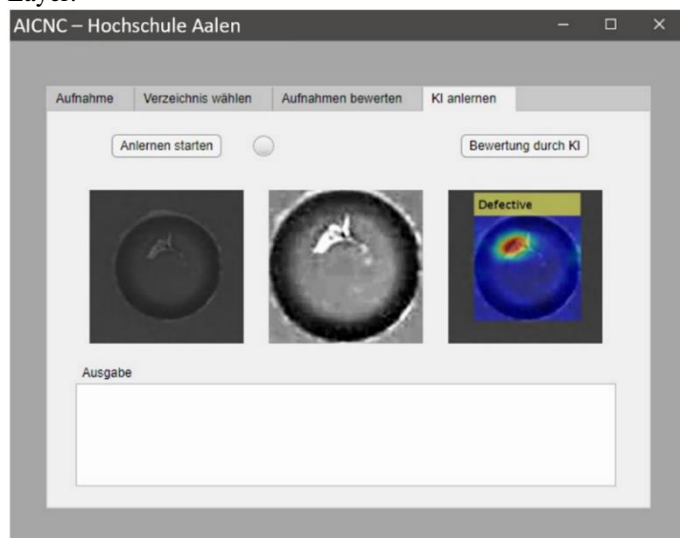


Fig. 9: Representation of the AICNC Teaching and Assessment tab

The input layer supports images as input with a resolution of 227 x 227 and three colour channels, i.e. for RGB images. The image is then convolved with a Convolutional Layer with 64 kernels with the dimensions 3 x 3. Behind the Convolutional Layers, there is a ReLU-activation function and then the output matrices are passed in a max-pooling layer. After that, there are

8 so-called Fire Modules. Each of these fire modules consists of a squeeze layer, an expand layer with a filter dimension of 1 x 1, and an expand layer with a filter dimension of 3 x 3.

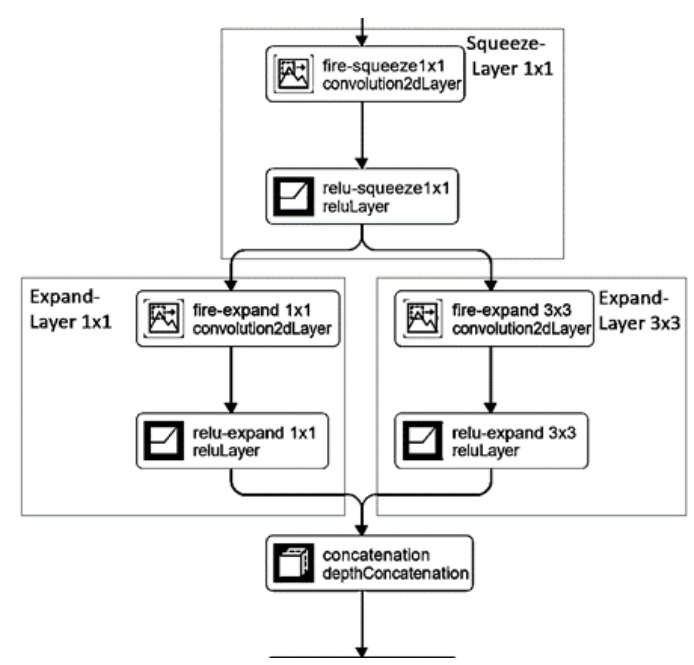


Fig. 10: The architecture of the Adapted Fire Module [10]

The squeeze net consists of a single convolution layer that reduces the number of input channels to a smaller value. This reduces the dimensionality of the input and allows for more efficient processing. The expansion process consists of a combination of 1 x 1 convolution layers and 3 x 3 convolution layers that increase the number of channels to a higher level. This combination allows complex features to be captured without requiring too many parameters.

After these fire modules follow another Convolutional Layer and a ReLU activation function, compare Fig. 10. A Global Average Pooling Layer follows this. A fully connected layer was added to the network structure. This consists of two layers, which reduces 1000 parameters to two parameters. From these parameters, the probabilities for the classes "good" and "defective" can be calculated with the help of the Softmax function [10].

Table II: The architecture of the adapted SqueezeNet DNN [10]

Layer Number	Layer Description		
1	Input Layer		
2	Convolutional Layer		
3	ReLU-Activation-Function		
4	Max-Pooling		
5	Fire Module 1		
6	Fire Module 2		
7	Max-Pooling		
8	Fire Module 3		
9	Fire Module 4		
10	Max-Pooling		
11	Fire Module 5		
12	Fire Module 6		

13	Fire Module 7
14	Fire Module 8
15	50% Dropout
16	Convolutional Layer
17	ReLU-Activation-Function
18	Global-Average-Pooling
19	Fully-Connected-Layer

In the presented use case, an ADAM-optimization function was used to optimize the learnable weights and bias parameters. ADAM-Optimiser is an optimization algorithm for the gradient descent method. ADAM is a further development of the RMSProb and AdaGrad optimizers. However, ADAM also incorporates momentum to improve convergence speed. After calculating the gradient g_t , the moving average of the first and second moments of the gradients is calculated:

$$m_t = \beta_1 * m_{t-1} + (1 - \beta_1) * g_t \tag{1.1}$$

$$v_t = \beta_2 * v_{t-1} + (1 - \beta_2) * g_t^2$$
(1.2)

 $\[mathcal{B}_1\]$ and $\[mathcal{B}_2\]$ are the decay factors for the moving average. The default values are used for $\[mathcal{B}_1=0.9\]$ and $\[mathcal{B}_2=0.999.$ Subsequently, this is used to calculate the bias-corrected first moment estimate:

$$\widehat{m}_t = \frac{m_t}{1 - \beta_1^t} \tag{1.3}$$

$$\hat{v}_t = \frac{v_t}{1 - \beta_2^t} \tag{1.4}$$

The updated parameters can now be calculated based on the following formula:

$$\theta_t = \theta_{t-1} - \frac{\alpha m_t}{\sqrt{v_t} + \epsilon} \tag{1.5}$$

 θ_t is the updated vector of parameters at time t. α corresponds to a fixed step size Element is a small value added to stability to avoid dividing by zero. The parameter update is divided by the adaptive learning rate using the corrected moment estimator and the square root of the corrected secondmoment estimator. The SqueezeNet was trained with a step size α of 0.0001. In addition, a learning rate schedule of a Drop factor of 0.7 every 10 epochs was added. An epsilon of 1e-8 was used [11]. A more detailed view at the network structure can be obtained in Fig. 13. The results of the DNN assessment are combined in the 'myNDNet-Postprocess' algorithm and superimposed on the corresponding pattern image. The superimposing process allows one to evaluate the results and identify spots with minor quality. The information is displayed to the user in a separate view, compared to Fig. 9. A blue coloration visualizes a good part. The change of colour from green to yellow to red symbolizes the increasing degree of damage. Red areas thus indicate defects on the workpiece.

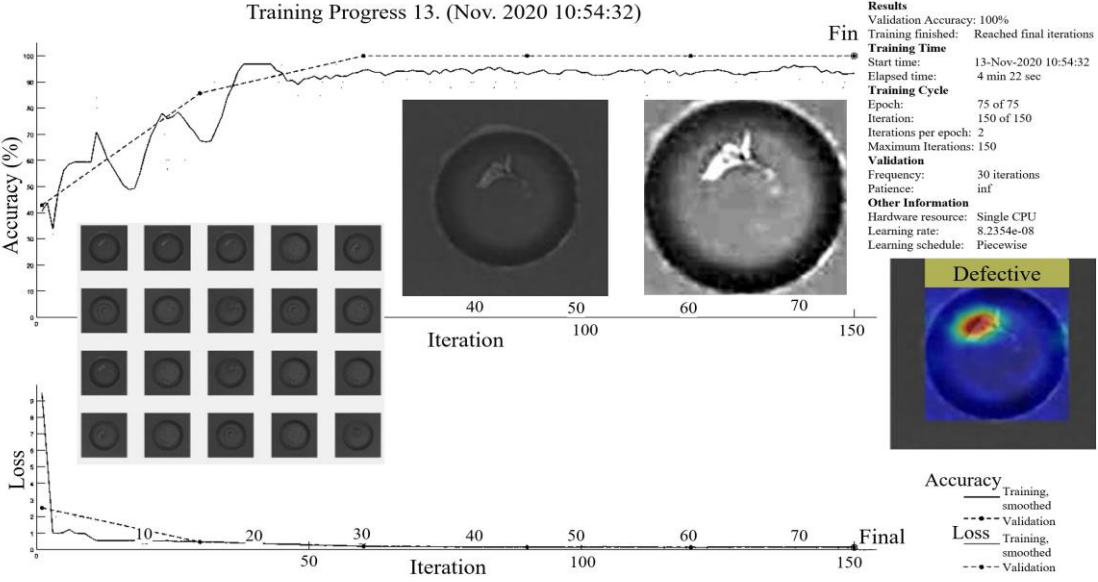


Fig. 11: DNN test pattern training progress and resulting defective test pattern layer activation map

Furthermore, this function provides the possibility to present and compare an image to a previously trained DNN classification result. Thus, the teaching process does not need to be repeated, and validation of the results can be assessed in minimum time. As mentioned, Fig. 9 right represents the

resulting DNN pre-processed test patterns in combination with the conclusion sensitivity map overlay. In the left area, the acquired sample pattern is visible on the right of the originated pattern file. The graphic on the right hand contains related user feedback on the AI classification result. It indicates whether the submitted milling workpiece is OK or NOK. In addition, the recursive activation layer image colours defective areas identified by the DNN. The dark red area of the activation layer image marks the defective part area. The visualization of the size and position of part defectives supports fast-track decision support, whether the part can be reworked or not.

IV. AICNC DNN ASSESSMENT WORK-FLOW

The AICNC workflow is divided into two separate processes. Initially, the DNN training procedure has to be performed. The training procedure during the development system tests is semi-automatised. The acquired test pattern is automatically cut into partial patterns that fit the demand of the DNN input network layer, compared to Fig. 10. The network structure is divided into the input layer, a hidden layer, and a fully connected layer. Finally, the class output is generated. The application of the used DNN originally targets object recognition tasks. Fig. 6 displays the reference pattern cuttings, including fully automatized centroid identification. The centroid identification algorithm automatically detects the weighted pattern centre based on the results of the canny edge detector algorithm, compared [12]. Fig. 6 right displays the corresponding pattern-cutting images automatically stored in the training folder by AICNC. The training images are named with increasing numbers. The training process demands a cluster of good and a cluster of defective images. With an increasing number of training images, the reliability of the DNN assessment results can be increased within the application of the tool within process usage. Fig. 12 displays the real-time visualization overlay of the camera-based perception user interface. For testing purposes, the trained DNN was additionally implemented in a consumer-market webcam device.



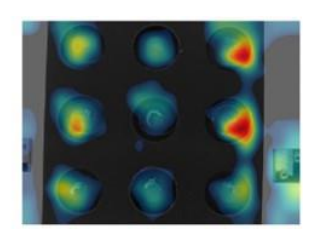


Fig. 12: DNN training procedure; left: Milled sample pattern sheet; right: perception-based real-time AI defect marking by recursive representation of the DNN layer activation

At least nine individual test patterns were needed within the experiment, to obtain an initial indication of the desired machine parameter settings. Fig. 12 left displays the milled test pattern (camera view), and Fig. 12 right represents the real-time camera view including activation map overlay. The camera is generating real-time class-activation map overlay (heat activation layer) with approx. 15-20 fps and indicates under the use of phased coloured fields, the occurring extends of part defectives. Areas with a high amount of edge and surface defects are marked with a dark red colour and indicate the degree of activation of the DNN layer according to the required features of the part.

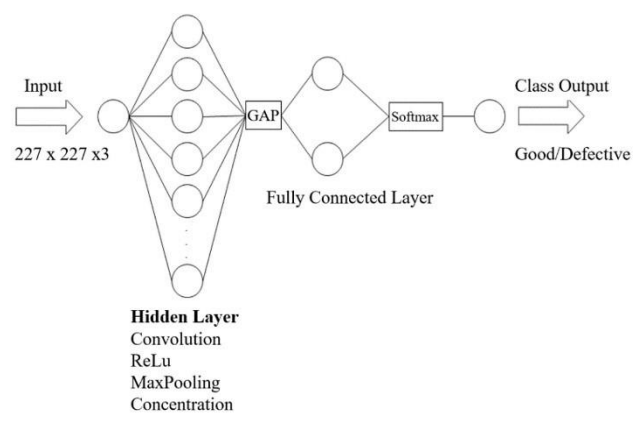


Fig. 13: AICNC – DNN layer structure, compare [5]

At this stage, the final system can provide reliable user feedback that indicates which areas may provide the optimal milling parameter set. The second column indicates that areas occur with insufficient activation of neurons. This leads to the demand to further harden the DNN with extended training data. Fig. 14 displays the assessed OK and NOK. sample parts. With the initial samples of 20 patterns, a validation accuracy of 60 % was reached under laboratory conditions. 20 % false assessed image patterns and 20 % with no correlation were achieved within the initial experiment. Nevertheless, not every sample pattern was classified correctly. Thus, further experiments must validate the usability of the system. Additionally, an increased database, generated within the industrial system-usage, will help to overcome classification problems. Additionally, different DNN structures will be tested to increase the testing accuracy. Fig. 14 represents the final assessment and labelling results by the AICNC-DNN.

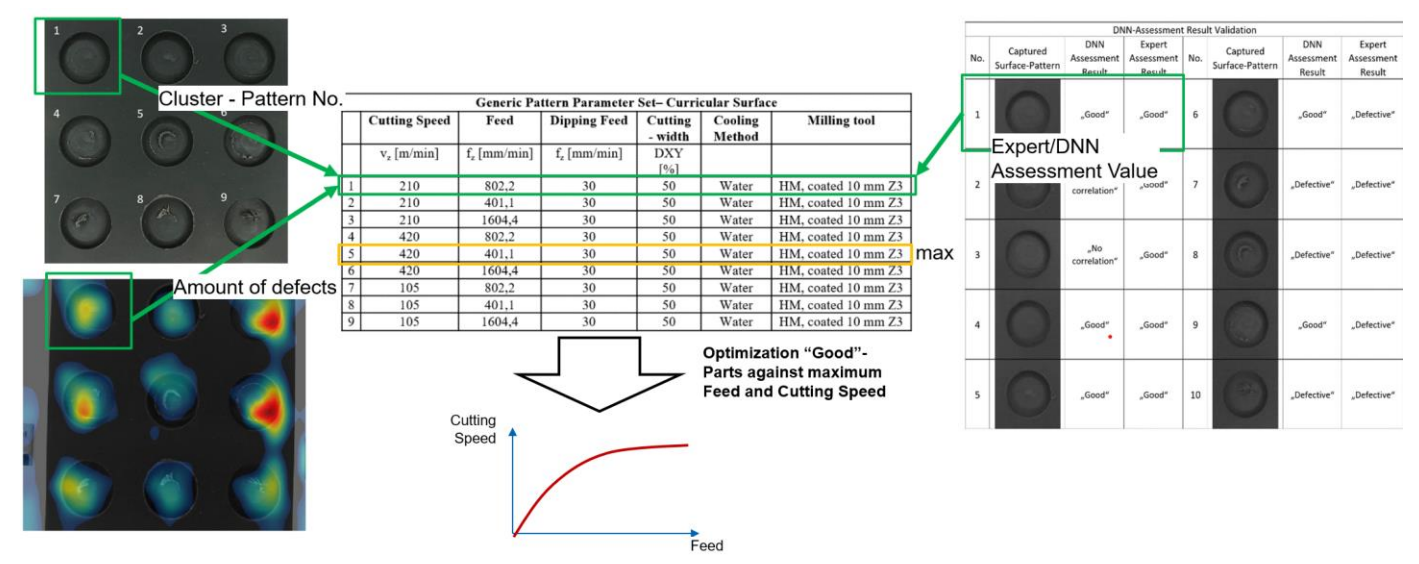


Fig. 14: Initial results of AICNC performance validation

V. CONCLUSIONS AND DISCUSSION

To validate the success of the DNN training at the initial training status, a random seed of 20 images of the category 'defective' was represented and assessed. At the current stage, the AICNC has been initially trained using a small number of test patterns. The test results from the perception-based real-time capturing device provide sufficient results to support milling parameter identification under industrial conditions. In future development steps, the AICNC will be trained under industrial conditions with an extended database. Furthermore, the network structure has to be replaced by the VGG-19 [13], a more specialized DNN structure. This network uses 19 layers and is also mainly used for object recognition. Internal tests have already shown better results under the use of different networks. That means that key users will use the software in customer projects.

ACKNOWLEDGMENT

The presented procedure results from research activities within the SimKI-Project 'Echtzeitdatenerfassung und Parameterkorrektur mittels einer mit Simulationsdaten angelernten KI'. The project was managed by Dr. Wolfgang Rimkus and Prof. Dr. Sebastian Feldmann. Funding was provided by the Ministry for Economy, Work and Housing in Baden-Württemberg (MFW) as part of the research programme 'KI Innovations Competition' in the year 2019.

REFERENCES

- [1] Sáenz de Argandona E., Aztiria A., Garcia C., AranaN., Izaguirre A., Fillatreau P. 'Forming processes control by means of artificial intelligence techniques'. Journal of Robotics and Computer-Integrated Manufacturing, 2008, doi: 10.1016/j.rcim.2008.03.014.
- [2] Europäische Kommission, 'Mitteilung der Kommission an das Europäische Parlament, den Europäischen Rat, den Europäischen Wirtschafts- und Sozialausschuss und den Ausschuss der Regionen: Green Deal der Europäischen Union', Brüssel, 2019

- [3] Romano P., 'European Manufacture of the Future, role of research and education for E European leadership', MANUFUTURE 2003 Conference, Italy, 2003.
- [4] Schlosser J. M., Schneider R., Rimkus W., Kelsch R., Gerstner F., Harrison D. K., Grant R. J., 'Material and simulation modelling of a crash beam performance – a comparison study showing the potential for weight savings using warm-formed ultra-high strength aluminium alloys', Journal of Physics, 2017, Vol. 896, pp. 12091, DOI 10.1088/17426596/896/1/012091
- [5] Feldmann S., Kempter G., Esslinger R., Tran H. T., 'Support of Image-Based Quality Assessment in Discrete Production Scenarios through AI-Based Decision Support', 13th International Conference on Advancements in Computational Sciences, ICACTE, 2020, ISBN: 978-1-4503-7732-4
- [6] Iandola F. N., Han S., Moskewicz M. W., Ashraf K., Dally W. J., Keutzer K., 'SqueezeNet: AlexNet-level accuracy with 50x fewer parameters and ¡0.5MB model size, 2016, arXiv:1602.07
- [7] [Online]. Available at: https://www.wirtschaft-digital-bw.de/ki-made-inbw/innovationswettbewerb-ki-fuer-kmu/simki-echtzeitdatenerfassungund-parameterkorrektur, 2020
- [8] 8. [Online] x-technik IT und Medien GmbH, 'DMU 65 monoBLOCK CNC universal milling machine'. [Online]. Available at: https:// https://www.zerspanungstechnik.com/bericht/horizontalbearbeitungszentren/dmu-65-h-monoblock_mit-bearbeitungszentrummaximal-flexibel-in-der-massenproduktion_2022-01-01, accessed in November 2022.
- [9] Hoffmann Group, Fraunhofer-Institut für Werkzeugmaschinen und Umformtechnik, 'Zerspanungshandbuch: Bohren, Gewinde, Senken, Reiben, Sägen, Fräsen, Drehen, Spanen, Präzisions-schleifen', 2. Aufl. München: Hoffmann Group, 2014, ISBN: 3-00-016882-6
- [10] Landola, Forrest N., et al. "SqueezeNet: AlexNet-level accuracy with 50x fewer parameters and< 0.5 MB model size." arXiv preprint arXiv:1602.07360 (2016).
- [11] Kingma, Diederik P., and Jimmy Ba. "Adam: A method for stochastic optimisation." arXiv preprint arXiv:1412.6980 (2014).
- [12] Rong W., Li Z., Zhang W., Sun L., An improved Canny edge detection algorithm, IEEE International Conference on Mechatronics and Automation, 2016, doi: 10.1109/ICMA.2014.6885761
- [13] Russakovsky, O., Deng, J., Su, H., et al. 'ImageNet LargeScale Visual Recognition Challenge', International Journal of Computer Vision (IJCV). Vol 115, Issue 3, 2015, arXiv:1409.0575v3
- [14] Feldmann, M. Schmiedt, J. M. Schlosser, W. Rimkus, T. Stempfle, C. Rathmann, 'Recursive quality optimisation of a smart forming tool under the use of perception-based hybrid datasets for training of a Deep Neural Network', Journal of Discover Artificial Intelligence, 2022, doi: 10.1007/s44163-022-00034-4